Light Gradients in Spherical Photosynthetic Vesicles

G. Paillotin,* W. Leibl,[#] J. Gapiński,[§] J. Breton,[#] and A. Dobek[§]
*INRA, 75338 Paris, France; [#]Section de Bioénergétique, DBCM, CEA Saclay, F-91191 Gif-sur-Yvette Cedex, France; and
[§]Institute of Physics, UAM, 61-614 Poznań, Poland.

ABSTRACT   Light-gradient photovoltage measurements were performed on EDTA-treated thylakoids and on osmotically swollen thylakoids (blebs), both of spherical symmetry but of different sizes. In the case of EDTA vesicles, a negative polarity (due to the normal light gradient) was observed in the blue range of the absorption spectrum, and a positive polarity, corresponding to an inverse light gradient, was observed at $\lambda = 530$ and $\lambda = 682$ nm. The sign of the photovoltage polarity measured in large blebs (swollen thylakoids) is the same as that obtained for whole chloroplasts, although differences in the amplitudes are observed. An approach based on the use of polar coordinates was adapted for a theoretical description of these membrane systems of spherical symmetry. The light intensity distribution and the photovoltage in such systems were calculated. Fits to the photovoltage amplitudes, measured as a function of light wavelength, made it possible to derive the values of the dielectric constant of the protein, $\epsilon_s = 3$, and the refractive index of the photosynthetic membrane for light propagating perpendicular and parallel to the membrane surface, $n_t = 1.42$ and $n_n = 1.60$, respectively. The latter two values determine the birefringence of the biological membrane, $\Delta n = n_n - n_t = 0.18$.

INTRODUCTION

A theory of light intensity distribution in systems of stacked planar layers, modeling the thylakoid membranes in chloroplasts, has been reported recently (Paillotin et al., 1993; Dobek et al., 1994; Gapiński et al., 1994). Equations derived from the theoretical considerations were applied to fit the experimental data obtained in photovoltage measurements based on the light-gradient effect. The theoretical studies have demonstrated the principles governing the experimentally observed wavelength dependence of the light-gradient photovoltage and, in particular, have explained the observation of inverted polarity upon excitation in a region of low absorption. Analysis of these results allowed us to estimate the chlorophyll concentration in the membrane, [Chl], the membrane thickness, L, and the distance between the stroma lamelle in a thylakoid, D. Values of the dielectric constants and refractive indices of the membrane and of the lumenal inner phase of the thylakoid were also obtained.

In general, photosynthetic systems do not have planar geometry, but some of them have spherical shapes and many others can be approximated by spheres. Examples of systems of such a spherical geometry are isolated bacterial chromatophores (Drews and Golecki, 1995), vesicles obtained from chloroplast thylakoids after special treatment (see Materials and Methods), native photosynthetic membranes of some species of bacteria (Imhoff, 1995), and liposomes with incorporated photosynthetic reaction centers or model systems (Steinberg-Yfrach et al., 1997). The size of these systems can vary from a few tens of nanometers up to micrometers.

Preliminary light-gradient experiments on spherical systems (small EDTA vesicles and large osmotically swollen thylakoids) have shown the occurrence of inversion of the photovoltage polarity depending on the wavelength of picosecond light pulses (Gapiński et al., 1995). In particular, at 530 nm, independently of the vesicle size, the inverse light gradient is detected. This observation cannot easily be explained within the earlier theory, which assumed antiparallel pairs of planar photosynthetic membranes and predicted an inversion only for certain well-defined values of the distance between the membranes. Therefore, it was desirable to develop a new theory that would describe 1) the propagation of light within systems of spherical symmetry (taking into account refraction and absorption); 2) the dipole moments induced by charge separation in the reaction center (RC), knowing the light distribution in such systems; and 3) the photovoltage generated in the light-gradient experiment measured by two electrodes at different positions along the light path within the suspension.

In this work we present data on the light-gradient photovoltage from small and large spherical vesicles prepared from chloroplast thylakoids. The data were obtained by excitation with a picosecond flash in the red absorption band at 682 nm, in the blue absorption band at 436 nm, and in a region of low absorption at 530 nm. The photovoltage elicited from large vesicles, of radius $r = 900$ nm, shows the same wavelength dependence of polarity as that observed for chloroplasts. Small vesicles, of radius $r = 110$ nm, exhibit a photovoltage response with a positive polarity (inverted light gradient) at 530 nm and at 682 nm, but with a negative polarity (normal light gradient) at 436 nm. In this work, the behavior of the light-gradient photovoltage amplitude and polarity will be explained by analysis of the light intensity distribution in pigmented spherical vesicles. We also present a new theoretical approach for systems in which the radius can take any value relative to the wave-

length, i.e., $r \leq \lambda$ and $r \geq \lambda$. It is shown that the experimentally found amplitude and wavelength dependence of the light-gradient photovoltage can be well simulated, assuming reasonable values for the refractive indices and dielectric constants of the membrane and surrounding aqueous medium, the chlorophyll concentration, and the thickness of the membrane.

MATERIALS AND METHODS

Preparation of EDTA vesicles

A stock solution of chloroplast thylakoids from spinach, obtained as described by Polle and Junge (1986) and Lill et al. (1986), was diluted to $10-30 \mu M$ chlorophyll in a solution containing $100 \mu M$ EDTA, 1 mM NaCl, and 1 mM HEPES (pH 7.8). The solution was incubated in the dark at room temperature for 20 min, after which NaCl was added to a final concentration of 30 mM to stop the incubation. The vesicles were centrifuged for 20 min at $30,000 \times g$ at $4°C$, and the pellet was resuspended in $100 \mu l$ of a medium containing 10 mM NaCl, 10 mM HEPES (pH 7.8), and 0.3 M sorbitol. The samples had a chlorophyll concentration of 0.65 mM and were stored on ice until use. The size of EDTA-treated thylakoids was analyzed by electron microscopy and light scattering spectroscopy. Both techniques showed that the average radius of such vesicles was ~ 100 nm.

Preparation of osmotically swollen thylakoids (blebs)

One hundred microliters of a stock solution of chloroplasts prepared as described by Polle and Junge (1986) and Lill et al. (1986) was resuspended in 30 ml of distilled water, incubated on ice for 12 h, and centrifuged at 15,000 RPM. The pellet, resuspended in $100 \mu l$ of distilled water (final chlorophyll concentration 0.68 mM), was used for the measurements. In the optical microscope, the blebs revealed diameters of $2-3 \mu m$.

Photovoltage measurements

The set-up for measuring the light-gradient photovoltage was essentially the same as the one described previously (Paillotin et al., 1993). A microcoaxial measuring cell (distance between the electrodes $100 \mu m$; Trissl et al., 1987a) was used for detection, and a Nd-YAG-driven Raman cell (Quantel, France) filled with pressurized H_2 was used for excitation. The concentration of the sample was adjusted to yield an optical density of $0.05 \leq OD \leq 0.5$ at the excitation wavelengths used. The photovoltage, attributed to photosystems I and II, was measured as a function of the flash energy, which yielded a saturation curve at each wavelength. The energy was expressed as the number of photons per cm^2, and the points from the initial slope of this curve were taken for further analysis.

THEORY

Source of the photovoltage

In the following, we assume that the photovoltage originates from the field of the electric dipoles created by the process of charge separation in the photosynthetic RC, an intrinsic membrane protein complex. The asymmetrical transmembrane organization of RCs makes charge separation reactions electrogenic. We further assume that, as for the chloroplast vesicles, the light distribution is inhomogeneous within the individual spherical vesicle. This light gradient is the source of anisotropy of the dipole moment distribution

in each sphere (Witt and Zickler, 1973; Fowler and Kok, 1974). The excitation light of intensity I_0 propagates in the measuring cell along the z direction, and the electrodes are positioned at different z. The induced voltage, V_{ph}, is equal to (Dobek et al., 1994; Gapiński et al., 1994)

$$V_{ph} = \frac{M^z_{sam}}{\epsilon \cdot \epsilon_0 \cdot S_z}, \qquad (1)$$

where M^z_{sam} is the value of the z component of the total sample dipole moment, S_z is the electrode surface normal to the z direction, and ϵ and ϵ_0 are the effective relative dielectric constant of the sample and the absolute dielectric constant of vacuum, respectively. The dipole moment, $\mathbf{M}_{sam}$, of the sample containing N_s identical independent spherical vesicles of radius r (see Fig. 1) is a sum of dipole moments, $\mathbf{M}_s$, created in each vesicle:

$$\mathbf{M}_{sam} = \mathbf{N}_s \cdot \mathbf{M}_s. \qquad (2)$$

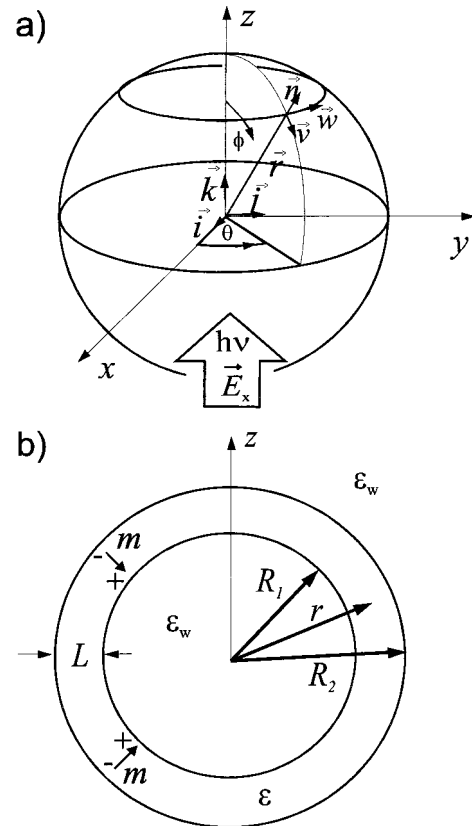FIGURE 1   (*a*) A schematic view of a spherical membrane whose center is at the origin of the Cartesian coordinates x, y, z (with unit vectors **i**, **j**, **k**) and the polar coordinates r, ϕ, θ (with unit vectors **n**, **v**, **w**). Light of intensity I_0 with its electric field vector $\mathbf{E}_0$ polarized in the x direction enters the system in the z direction. (*b*) Cross section of a single thin membrane separating two media of the same value of dielectric constant ϵ_w. $L = R_1 - R_2$ is the thickness of the membrane characterized by a complex dielectric constant $\epsilon = \epsilon_n(\mathbf{n:n}) + \epsilon_t(\mathbf{1 - n:n})$, and $r = R_1 + L/2$ is the radius for which the calculations are performed. The dipoles **m** are created in each reaction center perpendicular to the membrane.

For a single vesicle, M_s is a result of vector summation of N_d effective dipole moments, m^{eff}, induced in each excited RC of the photosynthetic membrane forming the vesicle:

$$M_s = \sum_{i=1}^{N_d} m_i^{eff}. \tag{3}$$

Using the arguments given before (Dobek et al., 1994; Gapiński et al., 1994; Trissl et al., 1987b), one can show that

$$m^{eff} = \frac{2 \cdot \epsilon_s + 1}{2 \cdot \epsilon_s + n_s^2} \cdot \frac{n_s^2 + 2}{3} \cdot m. \tag{4}$$

ϵ_s and n_s are the relative dielectric constant and the refractive index of the medium surrounding the dipole (protein), m, whose moment in vacuum is equal to

$$m = d \cdot e. \tag{5}$$

e is the electron charge, and d is the distance between the primary electron donor and the first electron acceptor. For the case where S is the surface of illuminated sample and for small values of OD, where $N_d \cdot N_s \cong I_0 \cdot S \cdot OD \cdot \ln 10$, one shows that the z component of the sample dipole moment, M_{sam}^z, can be expressed as

$$M_{sam}^z = N_s \cdot M_s^z = P^z(\lambda, r) \cdot I_0 \cdot S \cdot OD \cdot ln\,10 \cdot m^{eff}. \tag{6}$$

Here, $P^z(\lambda, r)$ is the fraction of light absorbed in the whole sphere, contributing to the z component of the sphere dipole moment M_s^z, and determining its sign.

Estimation of $P^z(\lambda, r)$ fraction of light absorbed in the sphere

Let us consider a medium of spherical symmetry, with the center of symmetry at 0. In addition to the Cartesian coordinates x, y, z with unit vectors i, j, k, we introduce the polar coordinates r, ϕ, and θ with unit vectors n, v, and w (Fig. 1 a). Let us consider incoming light of intensity I_0 with an electric field E_0 polarized linearly along the x axis and propagating along the z axis. In the following, the dielectric constant tensor of the medium is defined as

$$\epsilon = \epsilon_n(n{:}n) + \epsilon_t(1 - n{:}n), \tag{7}$$

where ϵ_n and ϵ_t are radial and tangential components of the ϵ tensor, respectively. Using the Maxwell equations, one looks for a solution of E, the electric field vector of light, in the form

$$E = nU + \nabla \cdot V + \nabla \times (nW), \tag{8}$$

where U, V, and W are functions of r, ϕ, and θ. E oscillates at $\omega = 2\pi c/\lambda$, the angular frequency corresponding to the wavelength λ, and c is the velocity of light in a vacuum. Let us introduce

$$k_n^2 = \frac{\omega^2}{c^2}\,\epsilon_n, \qquad k_t^2 = \frac{\omega^2}{c^2}\,\epsilon_t, \tag{9}$$

and:

$$\rho = k_t r, \qquad \eta = \frac{k_t^2}{k_n^2} = \frac{\epsilon_t}{\epsilon_n}. \tag{10}$$

Because the medium may absorb light, k_n and k_t can be complex numbers.

The angular dependence of U and W can be separated from the radial one and expressed in the form of sums of spherical harmonics, Y_l^m, where $l > 0$ and $-l \le m$ (integer) $\le +l$:

$$U(\rho, \phi, \theta) \approx \sum_{l=0}^{\infty} \sum_{m=-1}^{+1} Y_l^m(\phi, \theta) U_l(\rho), \tag{11a}$$

$$W(\rho, \phi, \theta) \approx \sum_{l=0}^{\infty} \sum_{m=-1}^{+1} Y_l^m(\phi, \theta) W_l(\rho). \tag{11b}$$

To solve Eq. 11, one looks for two particular independent solutions, $f_l(\rho, \eta)$ and $g_l(\rho, \eta)$. If $\eta = 1$ ($\epsilon_t = \epsilon_n$), $f_l(\rho, \eta)$ and $g_l(\rho, \eta)$ can be represented by spherical Bessel functions of the first kind, $j_l(\rho)$, and the second kind, $n_l(\rho)$ (Abramowitz and Stugen, 1972):

$$f_l(\rho, l) = \rho j_l(\rho), \qquad g_l(\rho, l) = \rho n_l(\rho). \tag{12}$$

The case of a single thin membrane

Let us consider the case of a single thin membrane separating two phases characterized by the same value of the dielectric constant ϵ_w (Fig. 1 b). The thickness of the membrane is $L = R_2 - R_1$, $R_1 \le r \le R_2$, $\rho = k_w r$, $\rho_1 = k_w R_1$, and $\rho_L = k_w L$. The dielectric constant of the pigmented membrane, ϵ, is complex and wavelength dependent; therefore, $\epsilon_n = \epsilon_n' + i\epsilon_n''$, and $\epsilon_t = \epsilon_t' + i\epsilon_t''$. Having defined $\delta_n = \epsilon_w/\epsilon_n - 1$ and $\delta_t = \epsilon_t/\epsilon_w - 1$, taking into account the boundary conditions and using the derived continuity equations, following the procedure given by Born and Wolf (1980), one can express the three components E_n, E_v, and E_w of the electric field E as

$$E_n = \sum_{l=1}^{\infty} \sqrt{-1}^{l-1} \frac{\epsilon_w}{\rho^2 \epsilon_n} (2l + 1) U_l(n\rho) P_1^{(1)}(\cos \phi)\cos \theta, \tag{13a}$$

$$E_v = -\sin \phi \cos \theta$$
$$\sum_{l=1}^{\infty} \sqrt{-1}^{l-1} \frac{\epsilon_w}{\rho \epsilon_t} \frac{(2l + 1)}{l(l + 1)} U_l'(n\rho) P_1^{(1)\prime}(\cos \phi) \tag{13b}$$
$$+ \frac{\cos \theta}{\sin \phi} \sum_{l=1}^{\infty} \sqrt{-1}^{l} \frac{k_w}{\rho} \frac{(2l + 1)}{l(l + 1)} W_l(n\rho) P_1^{(1)}(\cos \phi),$$

$$E_w = -\frac{\sin \theta}{\sin \phi} \sum_{l=1}^{\infty} \sqrt{-1}^{l-1} \frac{\epsilon_w}{\rho \epsilon_t} \frac{(2l+1)}{l(l+1)} U_l'(n\rho) P_1^{(1)}(\cos \phi)$$

$$+ \sin \theta \sin \phi \sum_{l=1}^{\infty} \sqrt{-1}^l \frac{k_w}{\rho} \frac{(2l+1)}{l(l+1)} W_l(n\rho) P_1^{(1)'}(\cos \phi),$$

(13c)

where $P_1^{(1)}(\cos \phi)$ is an associated Legendre polynomial, $P_1^{(1)'}(u) = d(P_1^{(1)}(u))/du$, where $u = \cos \phi$, and $U_l' = \partial U_l/\partial \rho$. The radial dependence of U_l and W_l is given by

$$U_l = \hat{j}_l(\rho) + (\rho - \rho_l)\delta_t \hat{j}_1^{(1)}(\rho) - \frac{\rho_L}{\rho_l^2} l(l+1)\delta_n \hat{h}_l \hat{j}_1^2$$

$$+ \rho_L \delta_t \hat{h}_1^{(1)} \hat{j}_1^{(1)} \hat{j}_\lambda,$$

(14a)

$$\frac{\epsilon_w}{\epsilon_t} U_l' = \hat{j}_1^{(1)}(\rho) + (\rho - \rho_l)\frac{l(l+1)}{\rho_l^2}\delta_n \hat{j}_l(\rho)$$

(14b)

$$-\frac{\rho_L}{\rho_l^2} l(l+1)\delta_n \hat{h}_l \hat{j}_l j^{(1)} + \rho_L \delta_t \hat{h}_1^{(1)} \hat{j}_1^{(1)} \hat{j}_1^{(1)2},$$

$$k_w W_l = \hat{j}_l(\rho) + \rho_L \delta_t \hat{h}_l \hat{j}_1^2. \qquad (14c)$$

In Eq. 14 $\hat{j}_l(x) = xj_l(x)$, $\hat{n}_l(x) = xn_l(x)$, $\hat{j}_1^{(1)}(x) = d \hat{j}_l(x)/dx$, and $\hat{h}_l(x) = xh_l(x)$, $\hat{h}_1^{(1)}(x) = d\hat{h}_l(x)/dx$, where $h_l(x) = n_l(x) \pm \sqrt{-1}j(x)$ is the spherical Bessel function of the third kind (Abramowitz and Stugen, 1972).

Light intensity

The expressions for the electric field amplitude allow a calculation of the normal, $I_n(\phi, \theta, r) = |E_n|^2$ and tangential, $I_t(\phi, \theta, r) = |E_v|^2 + |E_w|^2$, components of the total light intensity, $I(\phi, \theta, r)$, for given ϕ, θ, and ρ values (Paillotin, 1974). There, as the indices n, v, w correspond to the direction of $\mathbf{E}$ polarization, I_n and I_t are the intensity of the light beam propagating parallel and perpendicular to membrane surface, respectively. Their values averaged over all orientations and taken for a given ρ are

$$I_n(\rho) = \int_0^{2\pi} \int_0^{\pi} |E_n|^2 \sin \phi \, d\phi \, d\theta$$

(15a)

$$= 2\pi \frac{\epsilon_w^2}{\rho^4 |\epsilon_n|^2} \sum_{l=1}^{\infty} l(l+1)(2l+1)|U_l(\rho)|^2,$$

$$I_t(\rho) = \int_0^{2\pi} \int_0^{\pi} (|E_v|^2 + |E_w|^2)\sin \phi \, d\phi \, d\theta$$

(15b)

$$= \frac{2\pi}{\rho^2} \sum_{l=1}^{\infty} (2l+1)\left(\frac{\epsilon_w^2}{|\epsilon_t|^2}|U_l'(\rho)|^2 + |W_l(\rho)|^2 k_w^2\right).$$

Light absorbed in the layer

Given the distribution of light intensity in a layer, one can calculate P^z, the fraction of light intensity absorbed by a pigmented layer, which contributes to the induced electric dipole moment $\mathbf{M}_s$ in this layer. As stated before, it is assumed that $\mathbf{M}_s$ induced at a point indicated by r, is normal to the membrane. Then it can be shown that the fraction of light contributing to M_s^z, the z component of the dipole moment of the whole spherical layer, can be described by the relation

$$P^z(\lambda, r) = \int_0^{2\pi} \int_0^{\pi} (\epsilon_{n,1}'' I_n(\phi, \theta, r)$$

(16)

$$+ \epsilon_t'' I_t(\phi, \theta, r)) \sin \phi \cos \phi \, d\phi \, d\theta.$$

Taking into account the expressions obtained for the light intensity components and integrating Eq. 16 over the angles, one obtains

$$P^z(\lambda, r) = 4\pi \cdot \sum_{l=1}^{\infty} \text{Im} \frac{\epsilon_n'' \epsilon_w^2}{|\epsilon_n|^2} \frac{1}{\rho_l^4}\left(\frac{2}{\rho_l}\hat{j}_l - \hat{j}_l^{(1)}\right)l(l+1)(2l+1)$$

$$\cdot \left\{\delta_t(\rho - \rho_l)\hat{j}_l^{(1)} + \delta_n \frac{\rho_L}{\rho_l^2}l(l+1)\hat{h}_l \hat{j}_1^2 - \delta_t \rho_L \hat{h}_1^{(1)}\hat{j}_1^{(1)}\hat{j}_l\right\}$$

$$+ 4\pi \cdot \sum_{l=1}^{\infty} \text{Im} \frac{\epsilon_t''(2l+1)}{\rho_l^2}\left\{\left(\hat{j}_l - \frac{l(l+1)}{\rho_l^2}\hat{j}_l + \frac{1}{\rho_l}\hat{j}_l^{(1)}\right)\right.$$

$$\cdot \left[\frac{l(l+1)}{\rho_l^2}\delta_n \hat{j}_l(\rho - \rho_l + \rho_L \hat{h}_l \hat{j}_l^{(1)}) + \delta_t \rho_L \hat{h}_1^{(1)}\hat{j}_1^{(1)2}\right]$$

$$\left. - \left(\frac{1}{\rho_l}\hat{j}_l - \hat{j}_l^{(1)}\right)\delta_t \rho_L \hat{h}_l \hat{j}_1^2\right\}.$$

(17)

MODEL PREDICTIONS

To understand the generation of the dipole moment M_s^z in a spherical photosynthetic membrane, it is necessary to consider the light distribution in the system. A similar analysis was performed earlier, when light intensities were studied in two planar membranes simulating a thylakoid (Paillotin et al., 1993; Dobek et al., 1994). In pigmented spherical vesicles, the light gradient determining the photovoltage depends on the radius r, the membrane thickness L, and the wavelength λ (Eq. 17). But the theory not only allows a calculation of the fraction of the absorbed light contributing to M_s^z; it can also be used, e.g., to estimate the scattered and/or absorbed light intensity at any angle ϕ and θ in nonpigmented or pigmented spherical thin membranes (Fig. 1 a).

In the following we present model calculations (Figs. 2–6), which for demonstration are based on the set of geometrical, electric, and optical parameters determined for whole thylakoids (Dobek et al., 1994; Gapiński et al., 1994):
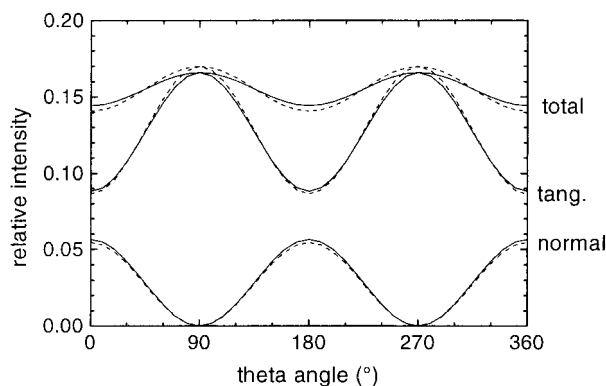
FIGURE 2   Values of the total I, normal I_n, and tangential I_t, components of light intensity calculated for $\phi = 45°$, $\lambda = 680$ nm, and two different sphere radii: $r = 25$ nm (——) and $r = 250$ nm (---), as a function of the θ angle. All intensity values were normalized to $I_0^\theta = \int_0^{2\pi} I(\theta)d\theta$. The polarized light in the x direction enters the sphere at $\phi = 180°$.

the refractive index of the medium outside and inside the vesicle, $n_w = 1.333$; the tangential and normal components of the refractive index of the membrane far from the absorption band, $n_m = n_t = n_n = 1.42$; the concentration of chlorophyll in the membrane, [Chl] = 0.45 M; and the thickness of the membrane, $L = 5.1$ nm. Two different vesicle radii, $r = 25$ nm and $r = 250$ nm, are chosen for presentation of the results. Calculation of both imaginary, $n''(\lambda)$, and real, $n'(\lambda)$, components of the membrane refractive index was performed on the basis of the absorption spectra of spinach thylakoid membranes, as described earlier (Paillotin et al., 1993; Dobek et al., 1994).

Taking for the radius of the spherical vesicle $r = R_1 + L/2$, one can obtain the light intensities I_n and I_t (Eq. 15) and the total intensity $I = I_n + I_t$ for different λ, r, ϕ, and θ. Fixing ϕ at a certain angle, one can calculate these intensities as a function of θ for a given r value and different λ. Fig. 2 shows that the θ dependence of the light intensities (calculated here relative to $I_0^\theta = \int_0^{2\pi} I(\theta)d\theta$, for example, for
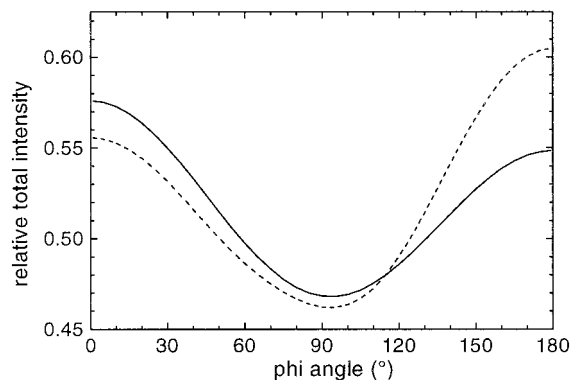

FIGURE 3   Values of the total light intensity $I = I_n + I_t$, calculated for $\theta = 45°$, $\lambda = 680$ nm, and two different sphere radii: $r = 25$ nm (——) and $r = 250$ nm (---), as a function of the ϕ angle. Light polarized in the x direction enters the sphere at $\phi = 180°$ (*from the right*). All intensity values were normalized to $I_0^\phi = \int_0^\pi I(\phi)\sin \phi \, d\phi$.
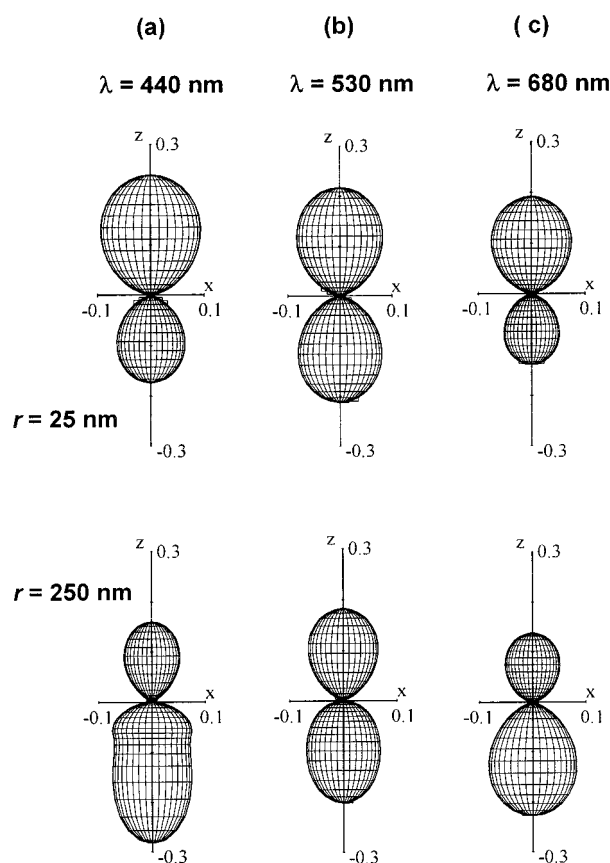

FIGURE 4   Light intensity distribution on the surface of a pigmented sphere, shown in arbitrary units as a 3D polar plot calculated from Eq. 15. To make the angular dependence more visible, only the deviation from the minimum value is presented, $\Delta I = I - I_{min}$. Calculations were performed for the sphere radii $r = 25$ nm and $r = 250$ nm. Incident nonpolarized light of wavelength $\lambda = 440$ nm, $\lambda = 530$ nm, and $\lambda = 680$ nm (*a, b, c,* respectively) enters the system along the z axis (*from the bottom*).

$\lambda = 680$ nm and linearly polarized light) is periodic with a period of π, as expected. For nonpolarized incoming light the oscillations disappear (not shown).

Of most interest here is the amount of light in the membrane at a given angle ϕ, which would allow a calculation of the z component of the induced dipole moment in the direction of the incoming light beam, and hence the measured photovoltage (Fig. 1 *a*). The ϕ-dependence of the light intensity relative to $I_0^\phi = \int_0^\pi I(\phi)\sin \phi \, d\phi$ was also calculated for two sphere sizes, $r = 25$ nm and $r = 250$ nm (Fig. 3). A simple comparison of the intensities on the poles indicates that there is in general an asymmetry of illumination of the upper hemisphere ($0 \leq \phi \leq 90$) when compared with that of the lower one ($90 \leq \phi \leq 180$; see Fig. 1 *a*). Depending on the radius, this asymmetry can be in favor of the entrance or exit side. If there is more light in the lower (the entrance) hemisphere with respect to the upper (the exit) one, we deal with a normal light gradient; otherwise the gradient is inverse.

The case of nonpolarized light of the wavelengths $\lambda = 440$ nm, $\lambda = 530$ nm, and $\lambda = 680$ nm is presented in Fig.
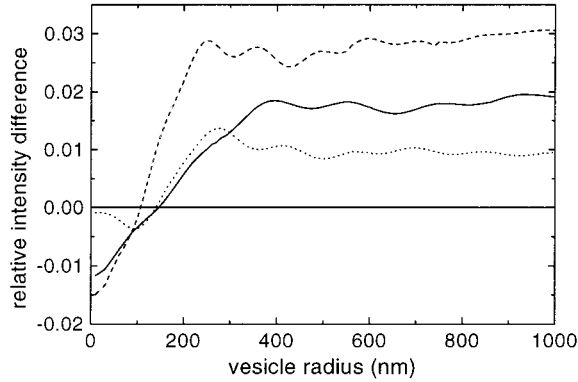
FIGURE 5 The difference, $\Delta I_{l,u} = I_l - I_u$, between the intensity I_l integrated over $90 \leq \phi \leq 180$ and I_u, the intensity integrated over $0 \leq \phi \leq 90$, calculated for fixed $\theta = 45°$, $\lambda = 440$ nm (– – –), $\lambda = 530$ nm (· · · · ·), and $\lambda = 680$ nm (——), as a function of radius r. Light polarized in the x direction enters the sphere at $\phi = 180°$. All intensity values were normalized to $I_0^\phi = I_l + I_u$.

4, which shows the light intensity distribution on the surface of a pigmented sphere as a 3-D polar plot in arbitrary units. It is calculated from Eq. 15 as a function of angles θ and ϕ for the radius $r = R_1 + L/2$ of two different vesicle sizes: $r = 25$ nm and $r = 250$ nm. To provide a better illustration, the minimum value, I_{min}, which, in all cases, is attained approximately at $\phi = 90°$ (see Fig. 3), was subtracted. The incident nonpolarized light enters the system along the z axis, from the bottom of the picture. As follows from the results shown in Fig. 4, where $I - I_{min}$ is depicted, the light distribution is different for the three wavelengths consid-
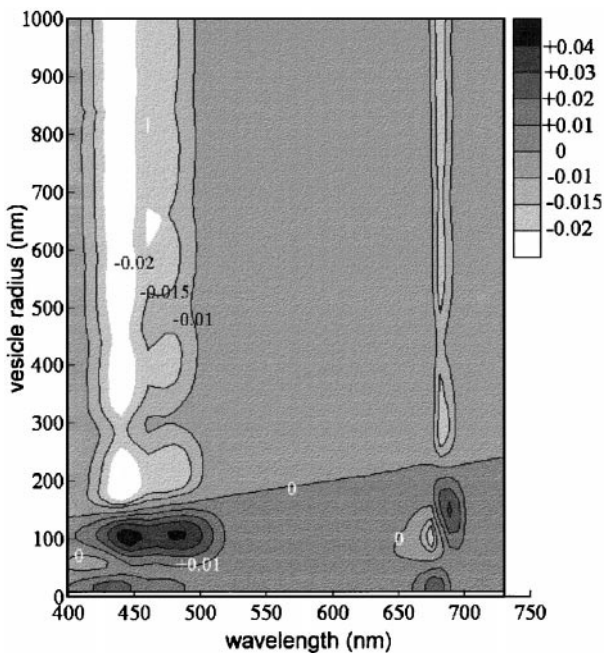

FIGURE 6 Contour plot of $P^z(\lambda, r)$, the fraction of light absorbed in the whole sphere, contributing to the z component of the sphere dipole moment, plotted as a function of wavelength λ and radius r. Positive values indicate an inverse light gradient, negative values a normal light gradient.

ered. The difference in volumes of the lower and the upper parts of the object reflects the light gradient created in the sphere. For a sphere of $r = 25$ nm, this difference is negative for the three tested wavelengths, indicating the inverse light gradient. For $r = 250$ nm, the normal gradient is noted for all wavelengths.

The difference of the intensities, $\Delta I_{l,u} = I_l - I_u$, where I_l indicates the integrated intensity in a lower semicircle ($90 \leq \phi \leq 180$) and I_u the integrated intensity in the upper semicircle ($0 \leq \phi \leq 90$), normalized to $I_0^\phi = I_l + I_u$ for fixed $\theta = 45°$, $\lambda = 680$ nm, $\lambda = 530$ nm, and $\lambda = 440$ nm as a function of radius r, is shown in Fig. 5. As indicated by this function for $r < \lambda/4$, an inverse light gradient is observed. A similar behavior of the dependence of light distribution on the distance between two membranes has been calculated at $\lambda = 680$ nm and $\lambda = 530$ nm for planar systems (see figure 4 in Dobek et al., 1994). For $r > \lambda/4$, the sign of $\Delta I_{l,u}$ changes. At $r \cong \lambda/2$, the value of $\Delta I_{l,u}$ reaches a maximum, and with its positive sign reflecting the normal gradient preserved, tends to a certain finite positive small value when the radius goes to infinity. Such a pattern of light distribution will create a nonzero component of the induced dipole moment in the z direction. The dependence of $\Delta I_{l,u}$ on the vesicle size suggests that light gradient measurements are sensitive to the radius of the sphere if $r \leq \lambda/2$.

Fig. 6 presents a dependence of the fraction $P^z(\lambda, r)$ (of light absorbed in the whole sphere, contributing to the z component of the sphere dipole moment; Eq. 17) as a function of the wavelength and radius in the form of a contour plot. The contour lines are drawn for identical values of $P^z(\lambda, r)$, which can be either positive or negative. As $P^z(\lambda, r)$ contributes to the z component of the dipole moment of the sphere, the obtained diagram permits a prediction of the resultant dipole moments induced by the light of a wavelength λ in a sample containing vesicles of the known radius r. It can be seen that large dipole moments will be induced in the membrane at wavelengths corresponding to the main absorption bands of chlorophyll for all tested parameters of the vesicles, except for a range of $r < 200$ nm, in which the inversion of polarization takes place. The parameter $P^z(\lambda, r)$ assumes a finite negative value for r tending to infinity, and the photovoltage created in spheres of very large radii is due to the normal light gradient.

COMPARISON WITH EXPERIMENTAL DATA

Taking into account Eqs. 1 and 6, the photovoltage V_{ph} induced between the two electrodes of the measuring cell is equal to

$$V_{ph} = \frac{P^z(\lambda, r) \cdot I_0 \cdot OD \cdot ln\, 10 \cdot m^{eff}}{\epsilon \cdot \epsilon_0}. \qquad (18)$$

To compare the experimentally obtained amplitudes and the theoretical values calculated from Eq. 18 for different wavelengths, it is convenient to normalize the photovoltage

data to the optical density, OD, of the sample; to the dielectric constant of the medium, ϵ; and to $Z = N \cdot \sigma(\lambda) \cdot I_0$, the number of absorbed photons per single photosystem, where $N = 300$ is the average antenna size in green plants (Simpson and Knoetzel, 1996), and $\sigma(\lambda)$ is the absorption cross section of a single chlorophyll molecule at a given wavelength. Then the normalized photovoltage of the sample is given by

$$\bar{V}_{ph} = \frac{V_{ph} \cdot \epsilon}{Z \cdot OD} = \frac{P^z(\lambda, r) \cdot \ln 10 \cdot m^{eff}}{\sigma(\lambda) \cdot N \cdot \epsilon_0}. \qquad (19)$$

Our measurements in suspensions of large and small vesicles were performed at three different wavelengths, $\lambda = 435.6$ nm, 530 nm, and 682 nm. Fig. 7 shows the wavelength dependence of the light-gradient photovoltage elicited from EDTA vesicle suspensions (Fig. 7 a) and osmotically swollen thylakoid (bleb) suspensions (Fig. 7 b), respectively, normalized as described above. In both cases the solid line represents the best fit calculated according to Eq. 19, with $n_n = 1.60$, and with r (EDTA vesicles) = 110 nm, and r (blebs) = 900 nm. The other parameters used for these calculations were $n_t = 1.42$, $n_w = 1.333$, $\epsilon = 40.8$, $L = 5.1$ nm, [Chl] = 0.45 M, $m^{eff} = |\mathbf{m}^{eff}| = 5.9 \cdot 10^{-28}$ C $\cdot$ m.

It is known from linear dichroism (LD) measurements that the photosynthetic membrane exhibits strong dichroism of absorption (Breton et al., 1973; Breton and Vermeglio, 1982). Using results of LD measurements, the tangential and normal components of the membrane dielectric constants and refractive indices were calculated (Fig. 8) (see also Discussion). For this purpose the dielectric constant values, fulfilling the relation $\epsilon_t''/\epsilon_n'' = DR(\lambda)$ in the spectral range of 650 nm $< \lambda <$ 730 nm, were used in the Kronig-Kramers transform, where $DR(\lambda)$ is the dichroic ratio value. To fit the measured photovoltage data, it was necessary, in addition, to assume a birefringence of the membrane, $\epsilon_n' =$

$\epsilon_t' + 0.55$. The value of $\epsilon_n' = 2.57$ obtained for the real part of the normal component of dielectric constant far from the absorption bands is in agreement with protein dielectric constant estimated recently for the bacterial reaction center ($\epsilon_s^0 = 2.5$; Krishtalik, 1995). To the best of our knowledge, the birefringence of a photosynthetic membrane has not been quantitatively determined until now, and this is the first report on the anisotropy of the refractive index (actually, its real part) in a biological membrane.

DISCUSSION AND CONCLUSIONS

In general, the complex refractive index of protein, water, and membrane suspension describes refraction and absorption in these media, and the analysis of our results required that the dispersion of ϵ and n be taken into account. Values of these parameters are frequency or measurement time dependent. For low frequencies, the real component of protein dielectric constant is indicated by ϵ_s, whereas for high frequencies, $\epsilon_s^0 = n_s^2$. The real part of the water complex dielectric constant is denoted as ϵ_w. Its value in the low-frequency range is higher than in the GHz frequency range, which is still higher than in the optical frequency range, where $\epsilon_w = n_w^2$.

The effective dielectric constant of the sample required for normalization of the photovoltage amplitude measured in the GHz range was calculated as before (Dobek et al., 1994; Gapiński et al., 1994). The dielectric constant of the suspension applied, $\epsilon = 40.8$, was lower than the value reported earlier, as a consequence of using a newly estimated value of the dielectric constant of H_2O, $\epsilon_w = 50$, measured in the GHz frequency range (Kim et al., 1994) and corresponding to our picosecond photovoltage measurements, instead of the value $\epsilon_w = 81$, which is valid for lower frequencies.
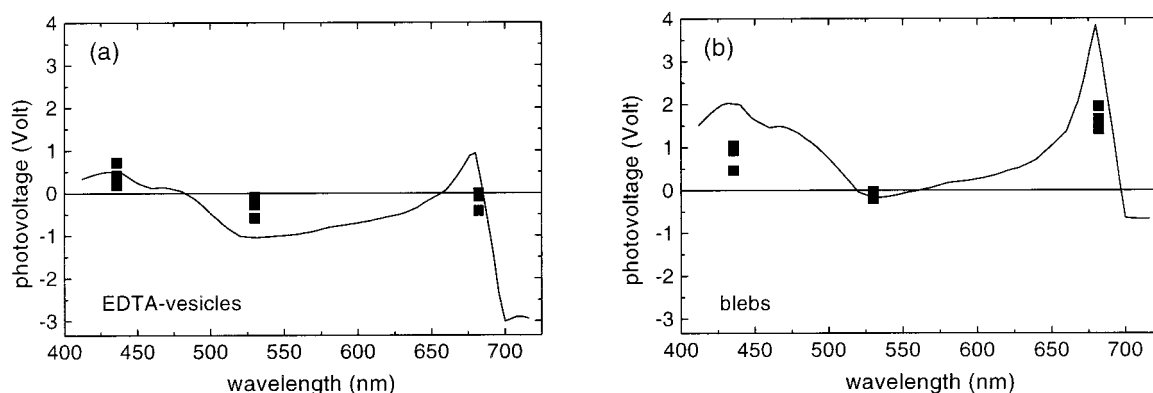

FIGURE 7   Wavelength dependence of the light-gradient photovoltage, $\bar{V}_{ph} = V_{ph} \cdot \epsilon/Z \cdot OD$, elicited from ($a$) spherical EDTA vesicle suspensions, (b) spherical osmotically swollen thylakoid (bleb) suspensions. Normalization is to the optical density OD, to estimated ϵ of the sample, and to $Z = N \cdot \sigma(\lambda) \cdot I_0$, the number of absorbed photons per single reaction center, where $N = 300$ is the average antenna size in green plants (Simpson and Knoetzel, 1996), and $\sigma(\lambda)$ is the mean absorption cross section of one chlorophyll molecule at a given wavelength. I_0 is the incoming light intensity. The solid line represents the best fit calculated according to Eq. 19, with $n_n = 1.60$ and $r = 110$ and $r = 900$, respectively. The other parameters used for the calculation were $n_t = 1.42$, $n_w = 1.333$, $\epsilon = 40.8$, $m^{eff} = 5.9 \times 10^{-28}$ C $\cdot$ m, $L = 5.1$ nm, [Chl] = 0.45M.
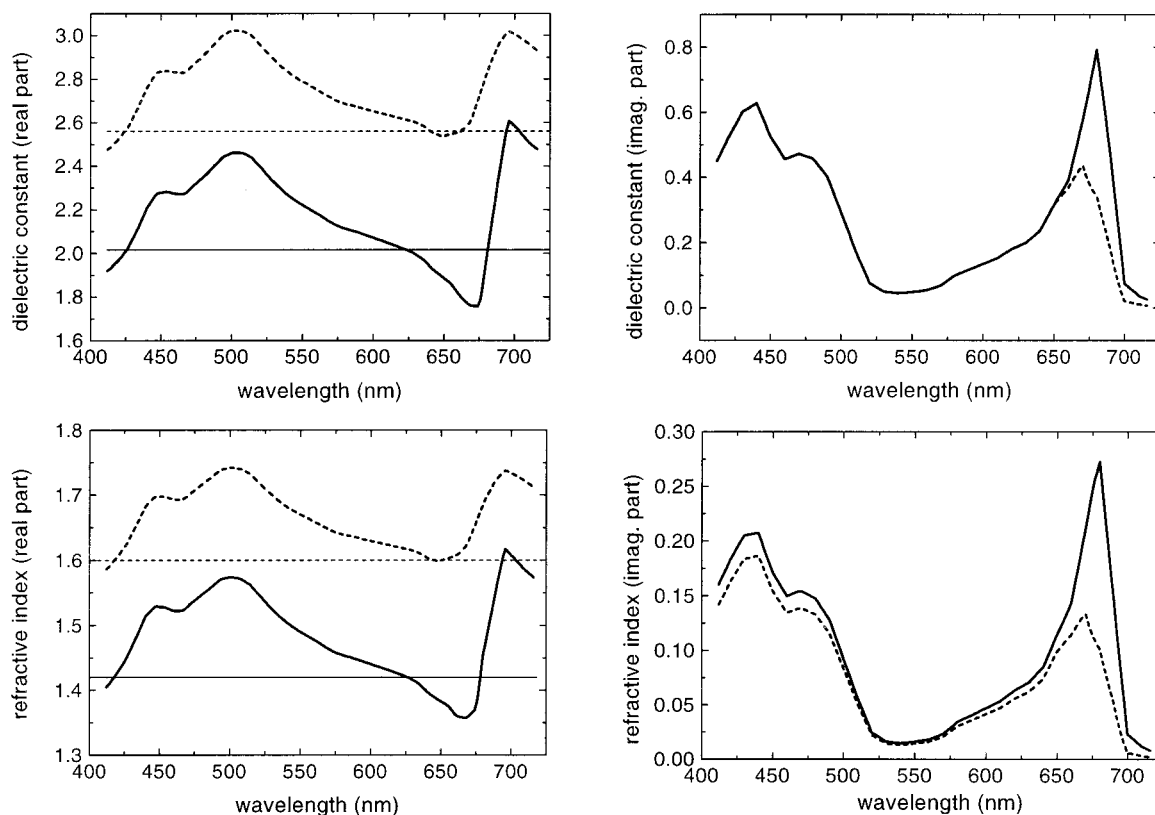
FIGURE 8   Normal (– – –) and tangential (——) components of real and imaginary parts of dielectric constants and refractive indices of photosynthetic membranes, calculated as described in the text.

For estimation of the effective dipole moment m^{eff}, the values of the relative dielectric constant $\epsilon_s = 3$ and refractive index $n_s = 1.58$ of the medium surrounding the dipole (Eq. 4) given by Krishtalik (1995) were applied. Both values, ϵ_s and n_s, were deduced from the analysis of different kinds of motions taking place in amino acid chains constituting the reaction center protein. The value $\epsilon_s = 3$ was found for the process having a characteristic time of 100 ps, typical of charge stabilization in a reaction center, whereas $\epsilon_s^0 = n_s^2 = 2.5$ describes the inertialess contribution to the effective dielectric constant in the optical range of frequencies.

When the refractive index for the light propagating perpendicular to the membrane surface ($\mathbf{E}_t$ parallel to it), $n_t = 1.42$, was taken into account, the fits of the photovoltage amplitudes measured as a function of wavelength and vesicle radius gave $n_n = 1.60$. The refractive index of the photosynthetic membrane, n_n, was indicated far from the absorption band for light propagating parallel to the membrane surface ($\mathbf{E}_n$ perpendicular to it). The parameters used in this calculation were the RC dielectric constant, $\epsilon_s = 3$ characteristic of the picosecond time range, membrane thickness $L = 5.1$ nm, molar chlorophyll concentration in the membrane, [Chl] = 0.45 M, and the effective dipole moment photogenerated in the RC, $m^{eff} = 5.9 \times 10^{-28} C \cdot m$.

In the case of EDTA vesicles, the positive polarity (due to the inversed light gradient) is observed in the blue range of the absorption spectrum. Negative polarity, reflecting the normal light gradient, is observed for $\lambda = 530$ and $\lambda = 682$ nm. Such a dependence of the photovoltage sign on the wavelength can be fitted with $r = 110$ nm (Fig. 7 a), assuming absorption anisotropy in the red region of the spectrum ($650 \leq \lambda \leq 730$). This assumption is in agreement with previous findings (Breton and Vermeglio, 1982) according to which, on the average, the transition moment for absorption at $\lambda = 680$ nm and longer wavelengths is oriented nearly in the plane of the membrane.

Recently, measurements of the polarized absorption and fluorescence performed at 77 K on preparation of trimeric light-harvesting complex II (LHC-II) from spinach have allowed a precise determination of the orientation angle of different absorbance transition dipoles (Van Amerongen et al., 1994). One monomer of LHC-II contains eight Chl a and six Chl b molecules, which have their chlorine rings roughly perpendicular to the membrane plane (Kühlbrandt and Wang, 1991; Kühlbrandt et al., 1994). Van Amerongen et al. (1994) showed that the strong absorption band around 676 nm was polarized essentially in parallel to the plane of the trimer aligned in the plane of the membrane. At $\lambda = 435.6$ nm and $\lambda = 530$ nm, the transition moments for absorption were much less dichroic, $\epsilon_t''/\epsilon_n'' = DR(\lambda) \cong 1$

(Breton et al., 1973; Breton and Vermeglio, 1982), which is also consistent with our data.

To obtain the best agreement not only as to the sign, but also to the amplitude of the photovoltage measured, a large anisotropy of the real part of the refractive index has to be assumed. We found that the birefringence of the photosynthetic membrane (the difference of refractive indices for the light propagating perpendicular and parallel to the membrane plane) estimated far from the absorption region was $\Delta n = n_n - n_t = 0.18$. The same difference was observed in the whole range of wavelengths studied for the real part of refractive indices. This is shown in Fig. 8, where the spectrum of the imaginary part is also presented. As far as we know, the dependencies of the normal and tangential components of the membrane refractive indices on the wavelength, taking into account the dichroism of absorption in the red range and the birefringence in the whole range of the spectrum, are reported here for the first time. The anisotropy of the refractive index leading to the birefringence of the photosynthetic membrane seems to be a general feature of biological membranes.

The results of the photovoltage polarity measured in large blebs (swollen thylakoids) are identical to the ones observed in whole chloroplast samples (Dobek et al., 1994), but the amplitudes are different. The calculations performed with Eq. 19 and the set of parameters discussed above fit the experimental results when the radius of the blebs is assumed to be $r = 900$ nm (Fig. 7 *b*). In the calculations no attempts were made to account for a size distribution of the EDTA vesicles or of the blebs. Nevertheless, the values of the radii obtained from the fits are in agreement with independent measurements of their average size (see Materials and Methods). Furthermore, the values of the imaginary parts of the normal and tangential components of the dielectric constant found in the red range of the photosynthetic membrane absorption spectrum (Fig. 8) support previous findings (Breton et al., 1973; Breton and Vermeglio, 1982). However, a distribution of the average vesicle size might well be responsible for the deviation between the experimental points and the calculated photovoltage curves in Fig. 7.

Recently, theoretical studies of spherical structures were applied to such systems as the Bragg reflectors and Fabry-Perot interferometer (Ping, 1994). The electromagnetic waves propagating in a single dielectric layer and in multiple dielectric layer systems with spherical geometry have been studied by the transfer matrix method. The source of the spherical wave was an infinitesimal current point at $r = 0$, and the electric field of propagating waves in such a system was described by $h_l^{(2,1)}(x)$, the spherical Bessel functions of the third kind. The smallest r_0 of the studied spheres was equal to λ_0, and this wavelength was used in the calculations as the dimension unit of the structure. The transmission and reflection of such a sphere as a function of the layer thickness (starting from $r_0/8$), the layer refractive index, and the frequency of transmitted wave were analyzed in ways compatible with our theoretical considerations.

The experimental results reported here on photosynthetic spherical vesicles indicate that the photovoltage induced in a suspension of whole chloroplasts (Trissl et al., 1987a, b) or in a suspension of photosynthetic bacteria (Deprez et al., 1986; Dobek et al., 1990, 1991) is not due to the geometrical anisotropy of these objects. Although observed in the objects with spherical symmetry, it proves that the intrinsic structure of a closed single photosynthetic membrane is responsible for this effect. The light distribution in a system of thin absorbing layers depends on three factors: absorption coefficients, refractive index differences, and the thickness of the layer with respect to the light wavelength (Paillotin et al., 1993; Dobek et al., 1994; Gapiński et al., 1994). We have shown that this also holds for a thin absorbing layer forming a spherical vesicle; however, the ratio of the sphere radius to the wavelength is also important. If we consider a light gradient in such a system, we find it sensitive to a change in any of these parameters.

REFERENCES

Abramowitz, M., and I. A. Stugen. 1972. Handbook of Mathematical Functions. Dover, New York.

Born, M., and E. Wolf. 1980. Principles of Optics. Pergamon, Oxford.

Breton, J., M. Michel-Villaz, and G. Paillotin. 1973. Orientation of pigments and structural proteins in the photosynthetic membrane of spinach chloroplasts: a linear dichroism study. *Biochim. Biophys. Acta.* 314: 42–56.

Breton, J., and A. Vermeglio. 1982. Orientation of photosynthetic pigments in vivo. *In* Photosynthesis: Energy Conversion by Plants and Bacteria, Vol. 1. Govindjee, editor. Academic Press, New York. 153–194.

Deprez, J., H.-W. Trissl, and J. Breton. 1986. Excitation trapping and primary charge stabilization in *Rps. viridis* cells measured electrically with picosecond resolution. *Proc. Natl. Acad. Sci. USA.* 83:1699–1703.

Dobek, A., J. Deprez, G. Paillotin, W. Leibl, H.-W. Trissl, and J. Breton. 1990. Excitation trapping efficiency and kinetics in *Rb. sphaeroides* R26.1 whole cells probed by transmembrane potential measurements in the picosecond timescale. *Biochim. Biophys. Acta.* 1015:313–321.

Dobek, A., W. Leibl, J. Breton, G. Paillotin, H.-W. Trissl, and A. Vermeglio. 1991. Kinetics of energy migration and trapping in the photosynthetic membrane of *Chloroflexus aurantiacus* as studied by photovoltage measurements. Proceedings of the Third Symposium on Inorganic Biochemistry and Molecular Biophysics and Sixth International Scientific School on Biological Macromolecules, September 15–21, 1991. Wroclaw-Karpacz, Poland. 177.

Dobek, A., G. Paillotin, J. Gapiński, J. Breton, W. Leibl, and H.-W. Trissl. 1994. Amplitude and polarity of the light gradient photovoltage from chloroplasts. *J. Theor. Biol.* 170:129–143.

Drews, G., and J. R. Golecki. 1995. Structure, molecular organization, and biosynthesis of membranes of purple bacteria. *In* Anoxigenic Photosynthetic Bacteria. R. E. Blankenship, M. T. Madigan and C. E. Bauer, editors. Kluwer Academic Publishers, Dordrecht, Boston, London. 231–257.

Fowler, C. F., and B. Kok. 1974. Rapid light induced potentials in spinach chloroplasts. *In* Progress in Photobiology. Proceedings of the Sixth International Congress on Photobiology, Bochum, 1972. G. O. Schenck, editor. Deutsche Gesellschaft f. Lichtforschung e.V., Frankfurt. 417.

Gapiński, J., A. Dobek, G. Paillotin, J. Breton, W. Leibl, and H.-W. Trissl. 1994. Light gradient in photosynthetic systems: theory and experiment. *Laser Physics.* 4:191–198.

Gapiński, J., G. Paillotin, W. Leibl, K. Gibasiewicz, J. Breton, and A. Dobek. 1995. Penetration of light in photosynthetic membranes of spherical symmetry. *In* Photosynthesis: From Light to Biosphere, Vol. 3. P. Mathis, editor. Kluwer Academic Publishers, Dordrecht, the Netherlands. 421–424.

Imhoff, J. F. 1995. Taxonomy and physiology of phototrophic purple bacteria and green sulfer bacteria. *In* Anoxigenic Photosynthetic Bacteria. R. E. Blankenship, M. T. Madigan, and C. E. Bauer, editors. Kluwer Academic Publishers, Dordrecht, the Netherlands. 1–15.

Kim, S.-H., G. Vignale, and B. DeFacio. 1994. Dynamic dielectric response function of liquid water. *Phys. Rev. A.* 50:4618–4624.

Krishtalik, L. I. 1995. Fast electron transfers in photosynthetic reaction centre: effect of the time-evolution of dielectric response. *Biochim. Biophys. Acta.* 1228:58–66.

Kühlbrandt, W., and D. N. Wang. 1991. Three-dimensional structure of plant light-harvesting complex determined by electron crystallography. *Nature.* 350:130–134.

Kühlbrandt, W., D. N. Wang, and Y. Fujiyoshi. 1994. Atomic model of plant light-harvesting complex by electron crystallography. *Nature.* 367:614–621.

Lill, H., S. Engelbrecht, G. Schonknecht, and W. Junge. 1986. The proton channel, CF_0, in thylakoid membranes. Only a low proportion of CF_1-lacking CF_0 is active with a high unit conductance (169 fS). *Eur. J. Biochem.* 160:627–634.

Paillotin, G. 1974. Étude théorique des modes de création, de transport et d'utilisation de l'énergie d'excitation électronique chez les plants superieures. Dissertation. Université Paris-Sud, Centre d'Orsay, Paris.

Paillotin, G., A. Dobek, J. Breton, W. Leibl, and H.-W. Trissl. 1993. Why does the light-gradient photovoltage from photosynthetic organelles show a wavelength-dependent polarity? *Biophys. J.* 65:379–385.

Ping, Er-Xuan. 1994. Transmission of electromagnetic waves in planar, cylindrical and spherical dielectric layer systems and their applications. *J. Appl. Phys.* 76:7188–7194.

Polle, A., and W. Junge. 1986. The slow rise of the flash-light-induced alkalization by photosystem II of the suspending medium of thylakoids is reversibly related to thylakoid stacking. *Biochim. Biophys. Acta.* 848:257–264.

Simpson, D. J., and J. Knoetzel. 1996. Light-harvesting complexes of plants and algae: introduction, survey and nomenclature. *In* Oxygenic Photosynthesis: The Light Reactions. D. R. Ort and C. F. Yocum, editors. Kluwer Academic Publishers, Dordrecht, the Netherlands. 493–506.

Steinberg-Yfrach, G., P. A. Liddell, S. C. Hung, A. L. Moore, D. Gust, and T. A. Moore. 1997. Conversion of light energy to proton potential in liposomes by artificial photosynthetic reaction centres. *Nature.* 385:239–241.

Trissl, H.-W., J. Breton, J. Deprez, and W. Leibl. 1987b. Primary electrogenic reactions of photosystem II as probed by the light-gradient method. *Biochim. Biophys. Acta.* 893:305–319.

Trissl, H.-W., W. Leibl, J. Deprez, A. Dobek, and J. Breton. 1987a. Trapping and annihilation in the antenna system of photosystem I. *Biochim. Biophys. Acta.* 893:320–332.

Van Amerongen, H., S. L. S. Kwa, B. M. van Bolhuis, and R. van Grondelle. 1994. Polarized fluorescence and absorption of microscopically aligned light-harvesting complex II. *Biophys. J.* 67:837–847.

Witt, H. T., and A. Zickler. 1973. Electric evidence for the field indicating absorption change in bioenergetic membranes. *FEBS Lett.* 37:307–310.